

## Quantitative Analysis of Hump Effects of Multi-Gate MOSFETs for Low-Power Electronics

Woojun Lee\* and Woo Young Choi

Dept. of Electronic Eng., Sogang Univ., 1 Shinsu-dong, Mapo-gu, Seoul 121-742, Korea.

Phone: +82-70-8285-8467 Fax: +82-2-705-8467 E-mail: \*lwj1026@sogang.ac.kr

### I. Introduction

Recently, for further improvement of performance, three-dimensional multi-gate MOSFETs have been investigated [1]. However, it was reported that multi-gate MOSFETs would suffer from a hump effect due to their non-planar channel structure which generates parasitic threshold voltages [2]. The hump effect increases off-current of MOSFETs because parasitic threshold voltages generally determine the sub-threshold characteristics of multi-gate MOSFETs as shown in Fig. 1. Thus, for low-power electronics, it is necessary to investigate the hump effect quantitatively.

In this paper, the accurate values of parasitic threshold voltages of multi-gate MOSFETs were extracted to evaluate the hump effect by using three-dimensional device simulation for the first time. Threshold voltages in each channel region were extracted by using the transconductance ( $g_m$ ) change method [3]. Also, the dependence of parasitic threshold voltages on the doping concentration of a fin and the radius of curvature of fin corners was studied.

### II. Parasitic Threshold Voltage Extraction

In order to confirm the validity of the transconductance change method for parasitic threshold voltage extraction, we assumed two parallel-connected single-gate planar MOSFETs, only whose gate workfunctions ( $\Phi$ ) and widths ( $W$ ) are different from each other as shown in Fig. 2.  $\Phi_n$  and  $W_n$  are defined as the gate workfunction and width of 'MOSFET  $n$ '. When ( $\Phi_1, \Phi_2$ ) and ( $W_1, W_2$ ) are (4.5, 4.9 eV) and (1, 10  $\mu\text{m}$ ), respectively, a hump is observed as shown in Fig. 3 (a). Fig. 3 (b) shows  $g_{m2}$  ( $=dg_m/dV_G$ ) as a function of the gate voltage ( $V_G$ ), which confirms that the transconductance change method successfully extracts threshold voltages of each MOSFET in that workfunction difference ( $\Delta\Phi$ ) is the same as threshold voltage difference ( $\Delta V_T$ ) extracted by the transconductance change method. Threshold voltages of MOSFET 1 ( $V_{T1}$ ) and 2 ( $V_{T2}$ ) are 0.616 and 0.814 V, respectively. However, as  $\Phi_2$  decreases from 4.9 to 4.7 eV, with  $\Phi_1$  fixed at 4.5 eV, the transconductance change method fails to extract threshold voltages of MOSFET 1 and 2 because one of the  $g_{m2}$  peaks disappears due to small  $\Delta\Phi$ .

In order to evaluate the accuracy of the proposed method, we defined the relative error of extracted threshold voltages with regard to  $\Delta\Phi$  as follows:

$$\text{Relative error (\%)} = 100(\Delta\Phi - \Delta V_T)/\Delta\Phi.$$

Fig. 4 (a) shows the relative error with the variation of  $\Delta\Phi$  and  $W_2/W_1$ . It turns out that as  $\Delta\Phi$  and  $W_2/W_1$  decrease, the relative error increases due to difficulty of  $g_{m2}$  peak sensing. However, as will be discussed in Section III, the transconductance change method is accurate enough to analyze hump effects of multi-gate MOSFETs. Also, it can extract threshold voltages of three parallel-connected MOSFETs as shown in Fig. 4 (b).

### III. Analysis of Hump Effects of Multi-Gate MOSFETs

In this section, the transconductance change method is introduced to analyze the hump effect of multi-gate MOSFETs quantitatively. Three-dimensional device simulation has been carried out by using ATLAS simulator [4]. Multi-gate MOSFETs such as tri-gate and gate-all-around (GAA) MOSFETs are considered for simulation as shown in Fig. 5. The dimensions of tri-gate and GAA MOSFETs are the same except for the existence of a bottom gate in GAA MOSFETs. The thickness of gate oxide is 4 nm. The width and height of a fin are 42 nm. Doping concentration of a fin is  $2 \times 10^{19} \text{ cm}^{-3}$ . The thickness of a buried oxide (BOX) layer is 50 nm. The workfunction of gate electrodes is 4.17 eV.

We extracted main threshold voltage ( $V_{T,\text{main}}$ ) and parasitic threshold voltages ( $V_{T,\text{corner}}$ ) of tri-gate and GAA MOSFETs by using the transconductance change method as illustrated in Fig. 6 (a). For the first time, it was observed that tri-gate MOSFETs have two different values of parasitic threshold voltages ( $V_{T,\text{corner}1}$  and  $V_{T,\text{corner}2}$ ) as illustrated in Fig. 6 (b). It results from the structural differences between upper and lower corners of a fin. Since the upper corners are controlled more strongly than the lower ones by the gate voltage,  $V_{T,\text{corner}1}$  is lower than  $V_{T,\text{corner}2}$ . However, in the case of GAA MOSFETs, only one parasitic threshold voltage ( $V_{T,\text{corner}}$ ) exists since there is no structural difference between upper and lower corners. To relieve the hump effect in three-dimensional MOSFETs, corner rounding and low fin doping concentration are used [6]. Fig. 7 (a) and (b) show the dependence of threshold voltages of tri-gate and GAA MOSFETs on fin doping concentration. As fin doping concentration decreases, each threshold voltage is observed to be converged into the same value-no hump. In the case of tri-gate MOSFETs,  $V_{T,\text{corner}2}$  is converged to  $V_{T,\text{main}}$  when the fin doping concentration is  $5 \times 10^{18} \text{ cm}^{-3}$ . Also, the hump effect is completely removed when the fin doping concentration is below  $1 \times 10^{18} \text{ cm}^{-3}$  both in the tri-gate and GAA MOSFETs. Fig. 8 (a) and (b) show threshold voltages as a function of the radius of curvature of fin corners. More than 16-nm radius of curvature is needed to suppress the hump effect when fin doping is  $2 \times 10^{19} \text{ cm}^{-3}$  both in tri-gate and GAA MOSFETs.

### IV. Summary

Transconductance change method is introduced to evaluate hump effects of multi-gate MOSFETs quantitatively for the first time. The effect of fin doping concentration and corner rounding on the hump effect is analyzed accurately. Since threshold voltages in each part of a multi-gate MOSFET can be extracted accurately, the proposed method will be very helpful low-power to multi-gate MOSFET design and compact modeling.

### Acknowledgements

Research for this publication was undertaken with the help of a Research Grant from Sogang University in the year 2008.

**Reference**

[1] S. Monfray *et al.*, *Symp. VLSI Tech. Dig.*, pp.108-109, 2002. [2] B. Doyle *et al.*, *Symp. VLSI Tech. Dig.*, pp.133-134, 2003. [3] W. Y. Choi *et al.*, *IEEE Trans. Elec. Dev.*, Vol. 51, No. 11, pp. 1833-1839. [4] SILVACO International, ATLAS User's Manual. [5] H. Hayt, *Engineering Electromagnetics*, McGraw-Hill, pp. 143-145, 2001. [6] W. Xiong *et al.*, *IEEE Int. SOI Conf.*, pp. 111-113, 2003.

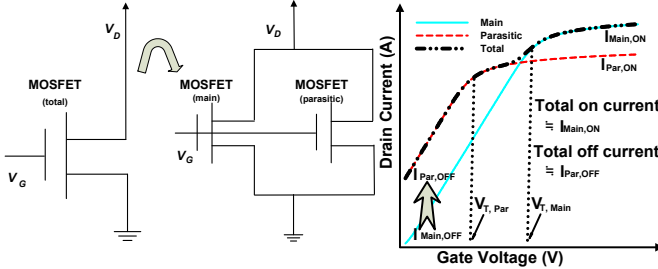


**Fig. 1.** Relationship between off-current and hump effects.

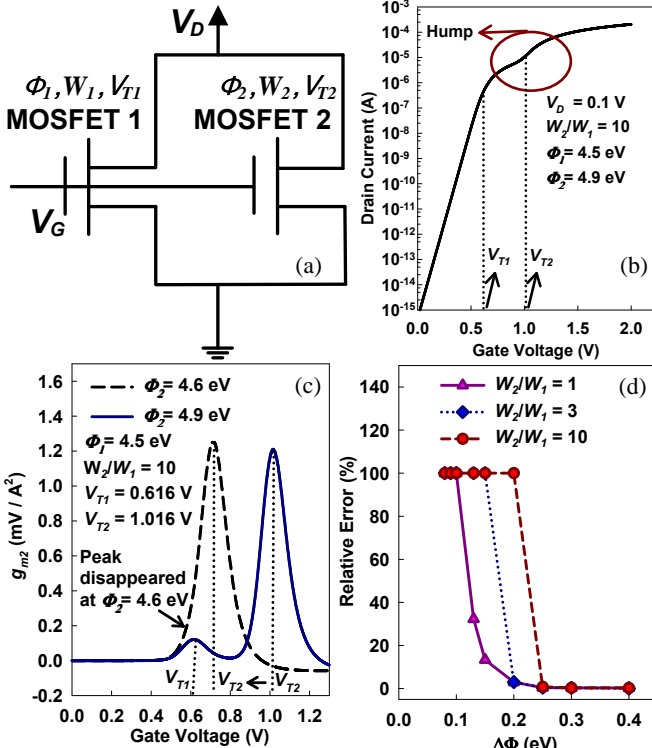


**Fig. 2.** (a) Parallel-connected single-gate MOSFETs. (b)  $I_D$ - $V_G$  curve. (c)  $g_{m2}$ - $V_G$  curves. (d) Relative error as a function of  $\Delta\Phi$ .

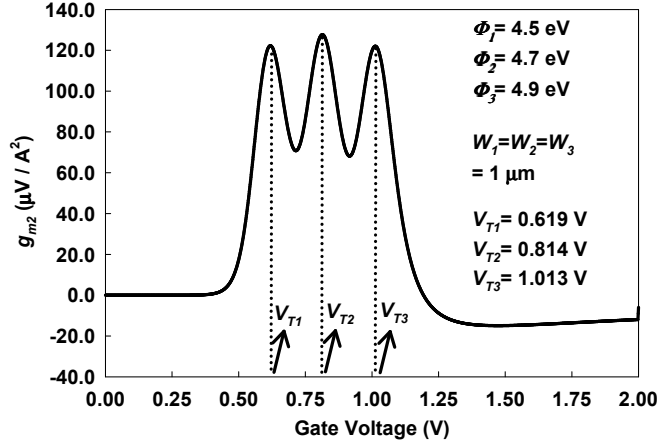


**Fig. 3.**  $g_{m2}$ - $V_G$  curve for three parallel-connected single-gate MOSFETs.

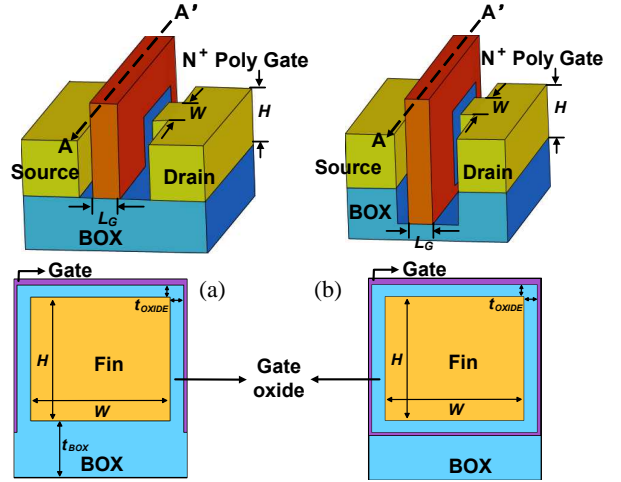


**Fig. 4.** Bird's eye and cross-sectional view (A-A') of (a) tri-gate MOSFETs and (b) GAA MOSFETs.

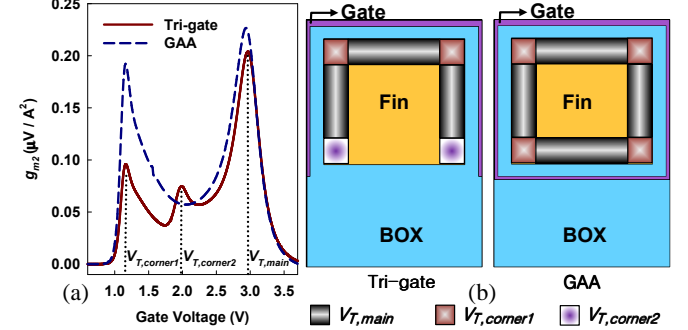


**Fig. 5.** (a)  $g_{m2}$ - $V_G$  curves and (b) cross-sectional view tri-gate and GAA MOSFETs describing regions of extracted threshold voltages.

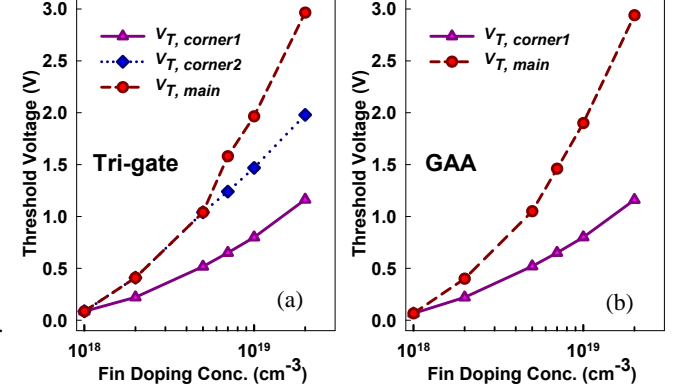


**Fig. 6.** Threshold voltages as a function of fin doping concentration of (a) tri-gate and (b) GAA MOSFETs.

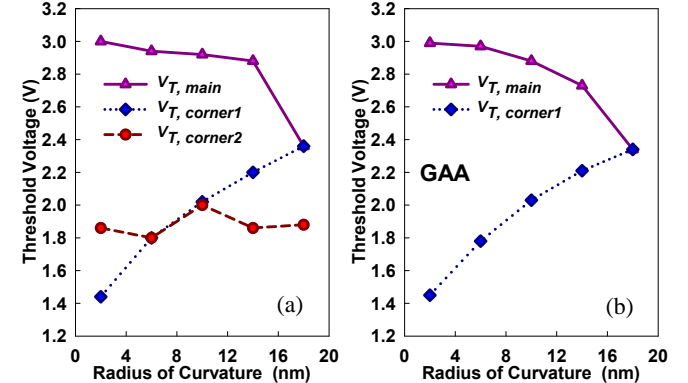


**Fig. 7.** Threshold voltages as a function of radius of curvature of (a) tri-gate and (b) GAA MOSFETs when fin doping is  $2 \times 10^{19} \text{ cm}^{-3}$ .